



HAL
open science

Semi-parametric Regression based on Machine Learning Methods for UAS Stall Identification

Vincent Guibert, Mathieu Brunot, Murat Bronz, Jean-Philippe Condomines

► **To cite this version:**

Vincent Guibert, Mathieu Brunot, Murat Bronz, Jean-Philippe Condomines. Semi-parametric Regression based on Machine Learning Methods for UAS Stall Identification. 19th IFAC Symposium on System Identification, Jul 2021, Padova (virtual), Italy. 10.1016/j.ifacol.2021.08.355 . hal-03286034

HAL Id: hal-03286034

<https://enac.hal.science/hal-03286034>

Submitted on 13 Jul 2021

HAL is a multi-disciplinary open access archive for the deposit and dissemination of scientific research documents, whether they are published or not. The documents may come from teaching and research institutions in France or abroad, or from public or private research centers.

L'archive ouverte pluridisciplinaire **HAL**, est destinée au dépôt et à la diffusion de documents scientifiques de niveau recherche, publiés ou non, émanant des établissements d'enseignement et de recherche français ou étrangers, des laboratoires publics ou privés.

Semi-parametric Regression based on Machine Learning Methods for UAS Stall Identification

Vincent Guibert ^{*,**} Mathieu Brunot ^{*} Murat Bronz ^{**}
Jean-Philippe Condomines ^{**}

^{*} ONERA – The French Aerospace Lab, 31055 Toulouse, France
(e-mails: vincent.guibert-ext@onera.fr, mathieu.brunot@onera.fr)

^{**} ENAC, Université de Toulouse, 31055 Toulouse, France
(e-mails: name.surname@enac.fr)

Abstract: A semi-parametric regression methodology is formulated to identify the unsteady lift characteristics of a small UAS undergoing dynamic stall. Based on the trailing edge separation model of Leishmann and Beddoes, the nonlinear evolution of the separation point is formulated so that it can be estimated by non-parametric Machine Learning methods. Validation of the methodology is presented with the identification of the lift coefficient based on quasi-steady wind tunnel tests.

Keywords: Nonlinear system identification, Machine learning, Grey box modelling, Unmanned aircraft system, Stall modelling, Non-parametric methods

1. INTRODUCTION

This paper investigates the estimation methods from the Machine Learning (ML) community and their potential benefits for the identification of a small Unmanned Aircraft System (UAS) stall model. ML is indeed an active field of research that is able to challenge the existing tools developed in system identification. It could be in particular extremely helpful for the ongoing certification and integration into civil airspace of UASs found in EU regulations (EU, May 2019), where arises a clear need for reliable full-envelope models of UAS flight dynamics, and in particular during upset situations (Cunis et al., 2019). Although the UAS community benefits from the full-scale aircraft identification experience, it has several specifics that may lead to different features compared to what could be expected from a regular transport aircraft. Regarding the stall phenomenon in particular, the low Reynolds number and the aerodynamic shape suggest a behaviour distinct from aircraft stall literature. The aim is therefore to consider ML tools to provide a picture of the physical phenomena involved.

Because flight dynamics and aerodynamic models have been studied in depth over the years, we do not consider here full black-box identification methods like for instance the Regression Trees (RT) in Kumar and Ghosh (2019). The idea is to keep the known parametric structure based on aerodynamic knowledge and to estimate the phenomenological part with a non-parametric method. Such an approach is usually referred to as semi-parametric regression – see e.g. Ruppert et al. (2003). The goal is to take advantage of ML tools for the non-parametric part, knowing that the parametric part is linear with respect to the coefficients. It should be noted that the authors made the choice to consider the ML tools here for a cultural

purpose rather than for technical reasons. In practice, methods not coming from the ML community may perform as well or better. In Janot et al. (2017), for instance, the authors successfully performed the semi-parametric identification of a robot with a State Dependant Parameter (SDP) estimation method.

Before diving into the stall modelling problem, the scope of the ML identification must be defined as ML tools cover an extensive range of problems. It is here intended to provide a non-parametric formulation for parts of the stall model based on dedicated tests. The training is therefore supervised. In addition, the limited size of the datasets recorded forces us to set aside deep learning tools and only consider regression techniques instead of classification ones. These restrictions lead us to consider three estimation methods: Support Vector Regression (SVR), Gaussian Process (GP) and Regression Trees (RT).

The paper is organized as follows: Sections 2 and 3 give overviews of stall modelling and ML methods respectively. They are combined in Section 4 to develop our solution which is evaluated on experimental data in Section 5. Finally, Section 6 provides concluding remarks.

2. STALL MODEL IDENTIFICATION

2.1 Stall Modelling

Small UASs are designed with increasing control performances that can quickly bring the aircraft to the limits of its flight envelop. Thus, it becomes mandatory to take into account many nonlinear aerodynamic phenomenons, such as stall. Stall is defined as the reduction of lift experienced by the aircraft as its angle of attack increases. The lift force, which is the component of the aerodynamic force

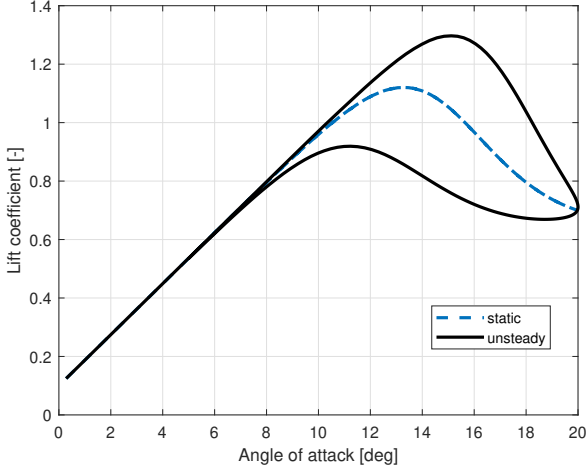


Fig. 1. Typical dynamic stall behaviour, based on (8)

orthogonal to the air velocity and in the symmetry plane of the aircraft, is given by

$$L = \frac{1}{2} \rho V^2 \cdot S \cdot C_L(\alpha, \dot{\alpha}, \dots) \quad (1)$$

where ρ is the air density, S the wing area, V the velocity relative to the air and C_L the lift coefficient. In particular, this lift coefficient houses all the non-linear effects as a function of its surface deflections (elevator, ailerons, flaps, etc.), landing gears position and its aerodynamic configuration (sideslip angle, angle of attack α and its derivative $\dot{\alpha}$, etc.). It is this relation that will be determined in this study, although for simplification, the dependence of the lift coefficient with respect to all but the angle of attack and its derivative will be neglected.

Stall arises from the flow separation caused by an adverse pressure on the upper surface of the wing. As such, the stall behaviour depends on the flight condition and the airfoil characteristics. Moreover, previous works (see *e.g.* Fischenberg (1995)) have shown that it can be divided into static and dynamic stall in the way shown Fig. 1. In the case of a non-steady flow, when the airfoil rapidly changes angle of attack for instance, the flow remains attached to the airfoil at a higher angle of attack than what was the case in steady conditions: stall appears delayed. Additionally, the same phenomenon is present on the way back when the aircraft is pitching nose down, where the flow reattaches at a lower angle of attack than in steady conditions, forming a hysteresis loop.

Since the first definition of dynamic stall, see *e.g.* McCroskey et al. (1976), numerous works have been conducted considering various airfoils and flow conditions. Amongst the various models developed, one can cite the semi-empirical Leishman-Beddoes model (Leishman and Beddoes, 1989), which is composed of four complementary modules to derive the unsteady lift, drag and pitch moment. Such a model is referred to as "semi-empirical" because one part derives from aerodynamic principles and the other is obtained by means of dynamic and static experiments. This study focuses on this model that is commonly used in the helicopter and wind turbine communities.

Table 1. Reduced frequency ranges

Range	Flow type
$k = 0$	steady
$0 < k \leq 0.05$	quasi-steady
$0.05 < k \leq 0.2$	unsteady
$k > 0.2$	highly unsteady

McCullough and Gault (1951) described three types of static stall at low speed (where the compressibility phenomena can be neglected):

- Trailing edge stall: the flow separation begins at the trailing-edge and the separation point moves forward;
- Leading edge stall: a sudden loss of lift after the burst of a leading edge laminar separation bubble;
- Thin airfoil stall: the flow separation begins at the leading-edge with reattachment and the separation point moves backward.

In Gault (1957), the author gives more elements regarding the stall type that can be expected from the airfoil shape and the Reynolds number.

2.2 Leishman-Beddoes Model

The complete Leishman-Beddoes model is divided in four sub-systems: unsteady attached flow, trailing edge flow separation, leading edge flow separation and vortex shedding (Leishman and Beddoes, 1989), where the use of empirical time constants and deficiency functions avoids the complex representation of viscous effects. In addition, according to Leishman (2006), the unsteadiness of the flow can be classified with the reduced frequency k given by

$$k = \frac{\omega \bar{c}}{2V} \quad (2)$$

where ω is the angular velocity and \bar{c} the mean aerodynamic chord. Table 1 relates the flow type to this reduced frequency. As an example, Fig. 1 is given for a quasi-steady flow with $k = 0.01$. Since the experimental results in Section 5 were obtained under quasi-steady flow condition, only the trailing edge flow separation sub-model will be considered here. The eventual leading edge flow separation, modelled by a delay in the onset of stall and where no change in behaviour is expected, is then encompassed by this model by maintaining a completely attached flow. This trailing edge flow separation is modelled using the Kirchhoff and Helmholtz theory

$$C_L = C_{L_0} + C_{L_\alpha} \left(\frac{1 + \sqrt{f}}{2} \right)^2 \alpha \quad (3)$$

where C_{L_0} is the zero angle of attack lift coefficient, C_{L_α} the attached lift curve slope and f is the flow separation point on the airfoil surface ($0 \leq f \leq 1$) such that the flow is attached with $f = 1$ and the separation is complete with $f = 0$. Leishman and Beddoes (1989) suggested to deduce the relationship between f and α from static tests.

As highlighted in Larsen et al. (2007), the negative point of the model (3) is the sensitivity of the lift coefficient with respect to the separation point:

$$\frac{\partial C_L}{\partial f} = \frac{1}{4} \left(1 + \frac{1}{\sqrt{f}} \right) C_{L_\alpha} \alpha \quad (4)$$

Because this sensitivity is infinite when the separation point approaches the leading edge ($f \rightarrow 0^+$), the estimation problem is most likely ill-conditioned. To avoid

this difficulty, Larsen et al. (2007) suggested the following transformation

$$2f = 1 + \cos(h) \quad (5)$$

such that when the separation point is at the trailing and leading edge, we have $h = 0$ and $h = \pi$ respectively. The lift coefficient can then be rewritten as:

$$C_L = C_{L_0} + C_{L_\alpha} \cos^4\left(\frac{1}{4}h\right) \sin(\alpha) \cdot \cos(\alpha). \quad (6)$$

Where as explained by Uhlig and Selig (2017), the trigonometric term for the lift curve slope C_{L_α} was replaced with $\cos(\alpha) \cdot \sin(\alpha)$ to be more consistent with the flat plate theory at high angles of attack. With the small angles assumption, the model (6) is equivalent to the original (3).

2.3 Parametric Stall

In Goman and Khrabrov (1994), the authors suggested that the separation point dynamic can be described by the following first-order ordinary differential equation:

$$\tau_1 \dot{f}(t) + f(t) = f_s (\alpha - \tau_2 \dot{\alpha}) \quad (7)$$

where τ_1 is the time lag corresponding to transient aerodynamic effects, τ_2 is the time lag of the flow separation/reattachment and f_s is the model for the steady-state separation. That function can be obtained in a non-parametric way from static wind tunnel measurements, as in Uhlig and Selig (2017).

An alternative solution, used for transport aircraft identification, is to parametrise f_s . One can cite the work of Fan and Lutze (1996) who developed a parametric model relying on an exponential function and including the pitch rate influence. Fischenberg (1995) proposed a model based on the *tanh* function such that

$$f_s = \frac{1}{2} (1 - \tanh [a_1 (\alpha - \tau_2 \dot{\alpha} - \alpha^*)]) \quad (8)$$

where a_1 is a shape parameter describing the abruptness of the transition and α^* is the angle of attack for $f = 1/2$. Fig. 1 depicts this model with $\tau_1 = 0.1s$, $\tau_2 = 0.3s$, $a_1 = 20rad^{-1}$, $\alpha^* = 15^\circ$ and $\alpha(t) = 10^\circ + 10^\circ \sin(\omega t)$ ($\omega = 0.67rad.s^{-1}$).

3. MACHINE LEARNING REGRESSION

It should be noted that the ML methods described here can be seen as parametric estimation approaches. Nonetheless, since they include many more parameters than the gray box models developed for stall modeling, we consider them as non-parametric solutions.

3.1 Support Vector Machine Regression

Support Vector Machine (SVM), developed by Vapnik (1995), consists in finding the optimal hyper-plane that deviates from the training points by a value no greater than a margin ϵ and which is as flat as possible. Though the method was originally dedicated to classification, it can be applied in a regression perspective. The method is said to be ϵ -insensitive because its goal is to minimize the following criterion

$$J(\mathbf{w}) = \frac{1}{2} \mathbf{w}^\top \mathbf{w} \quad (9)$$

s.t. $|y_i - f(\mathbf{w}, \mathbf{x}_i)| \leq \epsilon, \quad \forall i$

where \mathbf{w} is the parameters vector which regroups the coefficients defining the non-parametric function f to be estimated, $y_i \in \mathbb{R}$ and $\mathbf{x}_i \in \mathbb{R}^d$ are the dependent and independent variables respectively, both at sampling point i . Because it is possible that no such function f exists, the concept of soft margin is introduced such that the minimization problem becomes

$$J(\mathbf{w}) = \frac{1}{2} \mathbf{w}^\top \mathbf{w} + C \sum_{i=1}^N (\xi_i + \xi_i^*) \quad (10)$$

s.t. $\begin{cases} y_i - f(\mathbf{w}, x_i) \leq \epsilon + \xi_i, & \forall i \\ -y_i + f(\mathbf{w}, x_i) \leq \epsilon + \xi_i^*, & \forall i \\ \xi_i \geq 0, \quad \xi_i^* \geq 0, & \forall i \end{cases}$

where ξ_i and ξ_i^* are slack variables, C is the box constraint and N is the number of observations. In practice, the solution is easier to find in its Lagrange dual formulation.

The function f can either be linear with respect to the coefficients or nonlinear. In the latter case, one can use the kernel trick to implicitly map the data into a high-dimensional feature space function of the kernel where the regression problem becomes linear. To solve the quadratic problem, various dedicated algorithms have been developed such as the Sequential Minimal Optimization (SMO) (Fan et al., 2005).

3.2 Gaussian Process Regression

The stochastic process defined by $\{g(\mathbf{x}), \mathbf{x} \in \mathbb{R}^d\}$ is a Gaussian Process (GP) if the joint distribution of the random variables $g(\mathbf{x}_1), \dots, g(\mathbf{x}_N)$ is Gaussian. The mean value and the covariance functions of the GP are respectively defined as

$$\begin{aligned} E[g(\mathbf{x})] &= \mathbf{m}(\mathbf{x}), \\ \text{Cov}[g(\mathbf{x}), g(\mathbf{x}')] &= \mathbf{K}(\mathbf{x}, \mathbf{x}'). \end{aligned}$$

A GP Regression (GPR) model is defined such that

$$\forall i, \quad y_i = l(\mathbf{x}_i)\beta + g(\mathbf{x}_i) + \nu_i \quad (11)$$

where l is an explicit basis function, β is the vector of coefficients in this basis, g is a GP such that $g \sim GP(\mathbf{0}, \mathbf{K}(\mathbf{x}, \mathbf{x}'))$ and ν is the error term such as $\nu \sim \mathcal{N}(0, \sigma^2)$. The principle of this model, compared with an usual linear regression model, is to capture the smoothness of the response with the GP covariance function. This covariance function is represented by a kernel function parametrised by the coefficients γ . Therefore, the GPR, also called Kriging, has to estimate the feature space coefficients β , the noise variance σ^2 and the covariance hyper-parameters γ . This estimation is performed by optimizing a Maximum Likelihood criterion (Rasmussen and Williams, 2005).

3.3 Regression Trees

Classification And Regression Trees (CART) are decision tree algorithms dedicated to predictive modelling (Breiman et al., 1984). They are based on the principle of recursive partitioning. At each node of the tree, a test is performed on the independent variable \mathbf{x}_i and, depending on the result, the algorithm continues to one or another subbranch (one of two in the most common case of binary trees). Thus, the space of the independent

variables is successively divided into smaller regions, also called cells, that form a partition. To each cell is associated a terminal node, also called leaf, to which is assigned a numerical value in the case of CART. In classic regression trees, the value of the leaf L is simply the mean of the dependent measurements whose independent counterparts lie in the associated cell $y_L = \frac{1}{n_L} \sum_{i=1}^{n_L} y_i$ with n_L the number of such measurements. Thus, the resulting model is piecewise-constant. In order to split or merge the nodes, several rules are applied but the basic principle is to select the operation that minimises a given cost function such as the MSE. Various algorithms exist depending on the cost function, the selected optimizer and the stopping criterion.

4. SEMI-PARAMETRIC IDENTIFICATION

Based on the brief literature review on stall modelling from Section 2, the goal of the semi-parametric regression is to estimate both the vector $\boldsymbol{\theta} = [C_{L_0} \ C_{L_\alpha}]^\top$ on the parametric side and the relation defining the separation point $f(\alpha, \dot{\alpha})$ on the non-parametric side. Following the developments in Section 2.2, the formulation (6) is favoured to avoid the sensitivity issue when $f \rightarrow 0^+$. As has been seen Section 2.3, the non-parametric part of the model can be estimated beforehand based on dedicated static tests. Our objective is nonetheless to estimate both parametric and non-parametric components with one dynamic test in order to reduce the workload and the use of experimental facilities.

The following algorithm is then proposed:

- (1) **Initialization.** Select an initial estimate of the parameters $\hat{\boldsymbol{\theta}}_0 = [\hat{C}_{L_0} \ \hat{C}_{L_\alpha}]^\top$.
- (2) **Iteration.** The subscript i stands for the iteration number.
 - (a) Compute:
 - the static residuals
$$\epsilon_i(t) = C_L(t) - \hat{C}_{L_0},$$
 - the multiplicative components
$$\lambda_i(t) = \frac{\epsilon_i(t)}{\hat{C}_{L_\alpha} \cdot \sin \alpha(t) \cdot \cos \alpha(t)},$$
 - the pseudo-measurements
$$h_i^m(t) = 4 \cdot \text{acos}(\lambda_i(t)^{1/4}).$$
 - (b) Estimate the non-parametric model $\hat{h}_i(t)$ based on $h_i^m(t)$ with the selected ML method.
 - (c) Compute the new parametric coefficients $\hat{\boldsymbol{\theta}}_i$ based on (6) with the Least Squares method using the non-parametric estimate $\hat{h}_i(t)$.
 - (d) Check for convergence using the update on $\hat{\boldsymbol{\theta}}_i$.
- (3) **Convergence.** Compute the estimation error of the parametric component and construct the estimated separation point trajectory based on (5).

It would be tempting to estimate the multiplicative components directly in a non-parametric way. However, the coefficient C_{L_α} and the relation between the separation point and the angle of attack $f(\alpha)$ would then be unidentifiable.

Applying the algorithm above directly could however result in improper results due to non-respected constraints

of the problem arising from both errors in the initial estimates and the unconstrained nature of the ML tools. As such, the following two security mechanisms are implemented:

- A modification of the multiplicative components, $\bar{\lambda}_i$, to clip it in the range $[1/4, 1]$ in accordance with (3):

$$\bar{\lambda}_i(t) = \begin{cases} 1 & \text{if } \lambda_i(t) > 1 \\ 1/4 & \text{if } \lambda_i(t) < 1/4 \\ \lambda_i(t) & \text{otherwise} \end{cases}$$

- A capped value under the limit α_l , below which the stall is considered impossible to avoid issues arising from the division by "sin α · cos α " in $\lambda_i(t)$:

$$\bar{\bar{\lambda}}_i(t) = \begin{cases} 1 & \text{if } |\alpha| < \alpha_l \\ \bar{\lambda}_i(t) & \text{otherwise} \end{cases}$$

This new value $\bar{\bar{\lambda}}(t)$ is then the one used to compute the pseudo-measure $h_i^m(t)$ in step (2a) of the iterative algorithm.

5. EXPERIMENTAL RESULTS

5.1 Experimental Setup

The semi-parametric estimation is applied to experimental data from a single wing in a wind tunnel. As already stated, a single dependency on the angle of attack α and its change rate $\dot{\alpha}$ is assumed here. For the three non-parametric methods (SVR, GP and RT), the implementation of the Statistics and Machine Learning ToolboxTM of MATLAB[®] are used with default input parameters, with the exception of the SVR, where Gaussian kernel functions were used instead of the default linear ones. When available, the input data was standardised (SVR/GP).

Data was recorded during seven open wind tunnel experiments on a single aileron-less straight wing with NACA profile 0012, chord 0.15m and span 0.5m, placed perpendicular to the wind flow as to get no sideslip. The relative wind was generated constant and uniform for the duration of each experiment, while the angle of attack of the wing was progressively increased from 0° to 35° at a speed of approximately $10^\circ/s$ and back to 0° at $12^\circ/s$. Two wind velocities of 7.5m/s and 10m/s were tested, respectively with three and four experiments, and the wind velocity was sensed by a Pitot tube located ahead of the wing. This setup gives reduced frequencies between $k = 0.0013$ and $k = 0.0021$, positioning the experiment firmly in the quasi-steady domain. The lift coefficients C_L were derived from lift force measurements L and wind velocity V using (1). The data was recorded with a sampling frequency between 35Hz and 74Hz and then filtered by a second order Butterworth filter with a critical frequency of 1Hz.

During training, 20% of data selected at random was left out to be used for validation. It was chosen to select the validation dataset at random due to the small overall dataset (only seven, all different, experiments) where each experiment is susceptible to bring important information.

5.2 Global Stall Estimation

The hyper-parameter of the suggested methodology, α_l , was set to 6.5° . This value was chosen based on the data

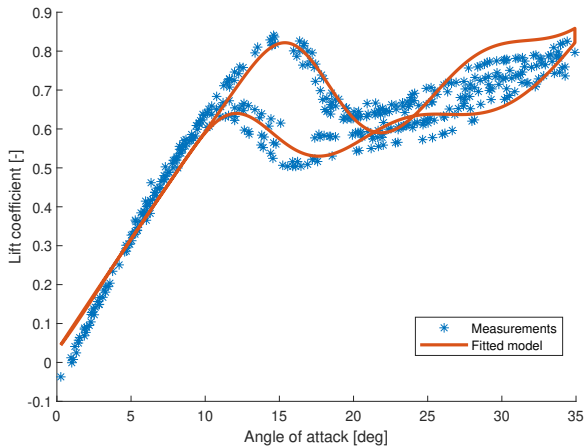


Fig. 2. Global model fitting using the SVR non-parametric method on the validation dataset

at hand and proved to be sufficiently low as to impact the process as little as possible while still efficiently filtering the low-alpha effect. Additionally, the initial parametric coefficients were set to $\hat{C}_{L_0} = -0.07$ and $\hat{C}_{L_\alpha} = 0.07\text{deg}^{-1}$ determined using the shape of the lift coefficient between 0° and 10° .

The first attempt is illustrated Fig. 2 for the SVR method. Immediately, one can note that the method seems to be biased in its estimate of the parametric coefficients. The parametric model being so simple, it can be reasonably assumed that the fault lies on the non-parametric ML learning of the separation point. Investigating the learnt relationship between the pseudo-measure $\hat{h}(t)$ and the abscissae $\alpha(t)$ and $\dot{\alpha}(t)$ indeed shows that the SVM regression with the default parameters fails to capture fine variations of the pseudo-measure. In addition, although the other two (not presented here for brevity) do not include this same bias they include strange artefacts reducing the overall precision of the fitted model, and in particular in proximity of the aerodynamic hysteresis. This second issue is attributed to the ML algorithms putting a greater than expected weight on the rate $\dot{\alpha}(t)$ due to the low variability of the measurements, since the experiments were conducted at quasi-constant rate and with only two values, one going forward and one going backward. The foreseen solution to this is to separate the problem into two sub-problems, respectively for the forward and backward motion and learn $h(t)$ as a function of the sole angle of attack $\alpha(t)$.

5.3 Separated Stall Estimation

Table 2 summarizes the results of this new method with each of its three variants by providing the computation time, the estimated parameters, as well as the Goodness of Fit (GoF) for both the estimated lift coefficient and separation point. It was chosen in this case to use for GoF the Normalized Root Mean Square Error (NRMSE) evaluated on the validation dataset.

As can be seen, the metrics indicate that the GP is the best fit of the three ML methods for our problem. It manages an impressive GoF of 94.08% on the validation dataset for the separation point, which translates into an

Table 2. Comparison of the separated stall estimation results for each of the ML methods

ML method	Execution time	Parameters		Validation GoF	
		\hat{C}_{L_0}	\hat{C}_{L_α}	C_L	f
SVR	13s	0.018	0.060	80.96%	91.34%
GP	12min37s	-0.054	0.074	88.04%	94.08%
RT	1min43s	-0.056	0.075	85.22%	92.66%

88.04% GoF on the lift coefficient. The RT method is closely behind with marginally lower GoFs and returned the same parametric coefficients, comforting the idea that both methods indeed reached the desired values. The RT is however more than seven times faster than the GP, an advantage one could leverage if there were a need for quick estimates and a continuous solution were not required. Finally, the SVR suffered from the same bias as in the previous test, returning different parameters than the two others which translated itself into strong differences in the learnt separation point. On top of that, the GoFs of SVR were still lower than that of the others, indicating that SVR with the parameters used in our example is not adapted (the authors would like to precise that one could very likely get usable results with properly selected SVR parameters but such parameters have so far eluded them).

Fig. 3 shows the results for the GP method. As noted before, the RT method yielded almost identical results, only with a non-continuous form (this result is presented Fig. 4). Although this result is very close to what was expected a few details must be discussed. First, at higher angles of attack the estimated flow separation point does not go all the way to 0 but rather reaches an asymptote of approximately 8%. This gap comes from neglected effects in the model that might not be able to precisely describe the behaviour of the particular wing used in our experiment at such angles of attack. Secondly, the behaviour of the estimated flow separation point on the forward path seems a bit odd in the interval $[6.5^\circ, 10.5^\circ]$, where it slowly decreases to 89% whereas the flow was expected to still be attached at this point. This is attributed once more to the model from (3), and particularly to its linear form at lower angles of attack. Our dataset indeed has a shape closer to that of a quadratic function with equation $C_L = -0.001743 \alpha^2 + 0.08813 \alpha - 0.07657$. Due to the process used, such an error is then necessarily transferred to the non-parametric estimator which integrates it in its learning, returning this result. These two shortcomings support the idea that although the model from Kirchhoff's theory is globally able to represent the behaviour of our wing one should be wary that the results might not be perfectly accurate. In addition, the shape of the separation point function in the $[10^\circ, 20^\circ]$ interval does not seem to follow a hyperbolic tangent form as expected from (8), furthering the idea that models from the literature may not be adapted to UASs.

6. CONCLUSION

In this paper, we utilized non-parametric regression methods from the Machine Learning (ML) community to help model the behaviour of a small UAS during stall while keeping a physical structure able to provide insight for aerodynamic engineers. The experimental results of the introduced methodology shows that:

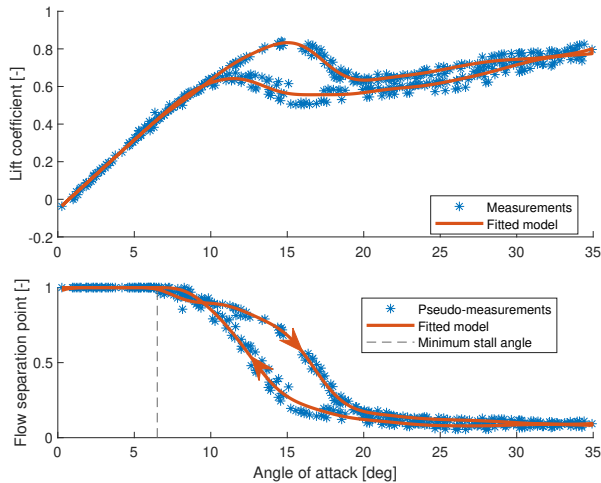


Fig. 3. Separated method fitting using the GP non-parametric method on the validation dataset

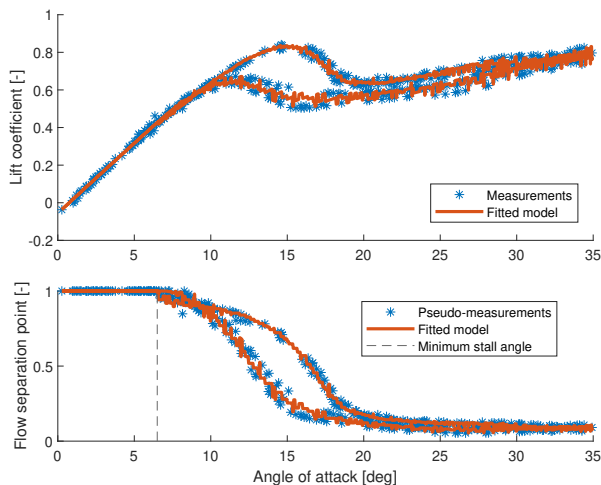


Fig. 4. Separated method fitting using the RT non-parametric method on the validation dataset

- ML methods are effective algorithms that benefit from being restrained to a subset of the problem based on physical analysis;
- A semi-parametric estimation of the dynamic stall can be performed with a single dynamic test.

Future work will address other aerodynamic coefficients and explore further the possibilities of ML methods with an evaluation of the hyper-parameters influence. In particular, the model should be confronted to separation point measurements to validate the non-parametric learning.

ACKNOWLEDGEMENTS

This work was supported by the Defense Innovation Agency (AID) of the French Ministry of Defense (research project CONCORDE N° 2019 65 0090004707501).

REFERENCES

Breiman, L., Friedman, J., Stone, C.J., and Olshen, R.A. (1984). *Classification and regression trees*. CRC press.

- Cunis, T., Burlion, L., and Condomines, J.P. (2019). Piecewise polynomial modeling for control and analysis of aircraft dynamics beyond stall. *Journal of Guidance, Control, and Dynamics*, 42(4), 949–957.
- EU (May 2019). Commission implementing regulation (eu) 2019/947 of 24 may 2019 on the rules and procedures for the operation of unmanned aircraft (text with eea relevance). *Official Journal of the European Union*, 2019.
- Fan, R.E., Chen, P.H., and Lin, C.J. (2005). Working set selection using second order information for training support vector machines. *Journal of machine learning research*, 6(Dec), 1889–1918.
- Fan, Y. and Lutze, F. (1996). Identification of an unsteady aerodynamic model at high angles of attack. In *21st Atmospheric Flight Mechanics Conference*, 3407.
- Fischenberg, D. (1995). Identification of an unsteady aerodynamic stall model from flight test data. In *20th Atmospheric Flight Mechanics Conference*, 3438.
- Gault, D.E. (1957). A correlation of low-speed, airfoil-section stalling characteristics with reynolds number and airfoil geometry. Technical Report TN-3963, NACA.
- Goman, M. and Khrabrov, A. (1994). State-space representation of aerodynamic characteristics of an aircraft at high angles of attack. *Journal of Aircraft*, 31(5), 1109–1115.
- Janot, A., Young, P.C., and Gautier, M. (2017). Identification and control of electro-mechanical systems using state-dependent parameter estimation. *International Journal of Control*, 90(4), 643–660.
- Kumar, A. and Ghosh, A.K. (2019). Decision tree- and random forest-based novel unsteady aerodynamics modeling using flight data. *Journal of Aircraft*, 56(1), 403–409.
- Larsen, J.W., Nielsen, S.R., and Krenk, S. (2007). Dynamic stall model for wind turbine airfoils. *Journal of Fluids and Structures*, 23(7), 959–982.
- Leishman, J.G. (2006). *Principles of helicopter aerodynamics*. Cambridge university press, 2nd edition.
- Leishman, J.G. and Beddoes, T. (1989). A semi-empirical model for dynamic stall. *Journal of the American Helicopter society*, 34(3), 3–17.
- McCroskey, W.J., Carr, L.W., and McAlister, K.W. (1976). Dynamic stall experiments on oscillating airfoils. *AIAA Journal*, 14(1), 57–63.
- McCullough, G.B. and Gault, D.E. (1951). Examples of three representative types of airfoil-section stall at low speed. Technical Report TN-2502, NACA.
- Rasmussen, C.E. and Williams, C.K.I. (2005). *Gaussian Processes for Machine Learning*. The MIT Press.
- Ruppert, D., Wand, M.P., and Carroll, R.J. (2003). *Semi-parametric regression*. 12. Cambridge university press.
- Uhlig, D.V. and Selig, M.S. (2017). Modeling micro air vehicle aerodynamics in unsteady high angle-of-attack flight. *Journal of Aircraft*, 54(3), 1064–1075.
- Vapnik, V.N. (1995). *The nature of statistical learning theory*. Springer.